

# Intermittent Hypoxia Mobilizes Bone Marrow-Derived Very Small Embryonic-Like Stem Cells and Activates Developmental Transcriptional Programs in Mice

Sina A. Gharib, MD<sup>\*1</sup>; Ehab A. Dayyat, MD<sup>2</sup>; Abdelnaby Khalyfa, PhD<sup>\*2,4</sup>; Jinkwan Kim, PhD<sup>2,4</sup>; Heather B. Clair, MSc<sup>2</sup>; Magdalena Kucia, PhD<sup>3</sup>; David Gozal, MD<sup>2,4</sup>

\*These authors contributed equally to the work

<sup>1</sup>Center for Lung Biology and UW Medicine Sleep Institute, Department of Medicine, University of Washington, Seattle, WA; <sup>2</sup>Department of Pediatrics, University of Louisville, Louisville, KY; <sup>3</sup>Stem Cell Biology Institute, University of Louisville, Louisville, KY; <sup>4</sup>Department of Pediatrics, University of Chicago, Chicago, IL

**Background:** Obstructive sleep apnea is a prevalent disorder associated with cognitive dysfunction and cardiovascular and metabolic morbidity and is characterized by recurrent episodes of hypoxia during sleep. Bone marrow-derived very small embryonic-like (VSEL) pluripotent stem cells represent a recruitable pool that may play an important role in organ repair after injury. We hypothesized that exposure to intermittent hypoxia (IH) can mobilize VSELs from the bone marrow (BM) to peripheral blood (PB) in mice and can activate distinct transcriptional programs.

**Methods:** Adult mice were exposed to IH or normoxia for 48 hours. VSELs were sorted from BM and PB using flow cytometry. Plasma levels of stem cell chemokines, stromal cell derived factor-1 (SDF-1), hepatocyte growth factor (HGF), and leukemia inhibitory factor (LIF) were measured. Transcriptional profiling of VSELs was performed, and differentially expressed genes were mapped to enriched functional categories and genetic networks.

**Results:** Exposure to IH elicited migration of VSELs from BM to PB and elevations in plasma levels of chemokines. More than 1100 unique genes were differentially expressed in VSELs in response to IH. Gene Ontology and network analysis revealed the activation of organ-specific developmental programs among these genes.

**Conclusions:** Exposure to IH mobilizes VSELs from the BM to PB and activates distinct transcriptional programs in VSELs that are enriched in developmental pathways, including central nervous system development and angiogenesis. Thus, VSELs may serve as a reserve mobile pool of pluripotent stem cells that can be recruited into PB and may play an important role in promoting end-organ repair during IH.

**Keywords:** Stem cells, sleep apnea, intermittent hypoxia

**Citation:** Gharib SA; Dayyat EA; Khalyfa A; Kim J; Clair HB; Kucia M; Gozal D. Intermittent hypoxia mobilizes bone marrow-derived very small embryonic-like stem cells and activates developmental transcriptional programs in mice. *SLEEP* 2010;33(11):1439-1446.

OBSTRUCTIVE SLEEP APNEA (OSA) IS A PREVALENT DISORDER IN CHILDREN<sup>1</sup> AND ADULTS<sup>2,3</sup> AND IS CHARACTERIZED BY THE OCCURRENCE OF repetitive episodes of airflow obstruction during sleep, leading to intermittent hypoxia (IH) and reoxygenation.<sup>4</sup> The morbid consequences of OSA are substantial and include cardiovascular, neurocognitive, and metabolic dysfunction.<sup>5-11</sup> For example, patients with OSA exhibit substantial memory and executive functional losses, have increased circulating markers of oxidative stress and inflammation, and develop regional gray matter loss.<sup>12-14</sup> In children, sleep apnea is associated with significant neurocognitive abnormalities, including attention deficits and poor school performance.<sup>15</sup>

Exposure to IH has now been widely used to model sleep apnea in animals,<sup>16,17</sup> and, while such model does not mimic all aspects of OSA, it recapitulates many of the pathophysiologic sequelae of OSA in humans, such as increased oxidative stress, hypertension and endothelial dysfunction, insulin resistance, and cognitive deficits.<sup>18-22</sup> To more closely approximate human

OSA, we and others have developed mouse models in which exposure to IH is applied only during periods of sleep and removed upon either arousal or wakefulness.<sup>17,23-25</sup> However, although recurrent hypoxia during sleep is a key characteristic of OSA, the molecular mechanisms by which IH promotes end-organ injury and, importantly, the responses mounted by the host to mitigate this effect remain poorly understood.

Accumulating evidence suggests that pluripotent stem cells residing in the bone marrow (BM) play an important role in the homeostasis and turnover of peripheral tissues and can be mobilized from the BM into the circulation during tissue injury and stress.<sup>26-30</sup> Recruitment of BM-derived stem-cell niches have been proposed as a major endogenous source for facilitation of structural and functional recovery, as well as promotion of the regeneration of damaged organs.<sup>31,32</sup> Ratajczak et al.<sup>33</sup> have recently identified a homogenous population of rare, small ( $\sim 3.7 \mu\text{m}$ ) pluripotent stem cells residing in murine BM that express cellular markers characteristic for embryonic lineage and have shown that such stem cells can differentiate into lineage-committed cells from all 3 germ layers. Indeed, Sca-1<sup>+</sup> Lin<sup>-</sup> CD45<sup>-</sup> very small embryonic-like stem cells (VSELs) can be mobilized from the BM to peripheral blood (PB) in response to specific chemokine gradients, including stromal cell-derived factor-1 (SDF-1), hepatocyte growth factor (HGF), and leukemia inhibitory factor (LIF).<sup>33,34</sup> We have previously reported on the recruitment of VSELs from BM to PB following tissue-specific injury, including stroke<sup>30,35</sup> and myocardial infarction.<sup>27,29</sup> In the present study, we hypothesized that mice

---

Submitted for publication May, 2010

Submitted in final revised form June, 2010

Accepted for publication June, 2010

Address correspondence to: David Gozal, MD, Department of Pediatrics, 5721 S. Maryland Avenue, MC 8000, Suite K-160 Chicago, IL 60637; Tel: (773) 702-6205; Fax: (773) 702-4523; E-mail: dgozal@peds.bsd.uchicago.edu

exposed to IH will increase plasma levels of stem cell-specific chemoattractants and mobilize BM-derived VSELs into the PB. Furthermore, since these pluripotent stem cells possess the ability to differentiate into any cell type, we performed gene expression profiling to systematically map the transcriptional architecture of activated programs within VSELs in response to IH.

## MATERIALS AND METHODS

### Animals

Adult male mice (2 months old), C57BL/J6, were purchased from Jackson Laboratory (Jackson Laboratory, Bar Harbor, ME). All animal experiments were performed according to protocols approved by Institutional Animal Care and Use Committee of the University of Louisville and complied with the American Physiological Society Guidelines for Animal Studies.

### Exposure to IH

Mice were placed in 4 identical commercially designed chambers ( $30 \times 20 \times 20$  in.; Oxycycler model A44XO; Biospherix, Redfield, NY) that were operated under a 12-hour:12-hour light-dark cycle (07:00 -19:00) for 48 hours. Gas was circulated around each of the chambers, attached tubing, and other units at 60 L/min (i.e., 1 complete change/10 s). The O<sub>2</sub> concentration was measured continuously by an O<sub>2</sub> analyzer and was changed using a computerized system controlling the gas valve outlets such that the moment-to-moment desired O<sub>2</sub> concentration of the chamber was programmed and adjusted automatically. Deviations from the desired concentration were met by addition of N<sub>2</sub> or O<sub>2</sub> through solenoid valves. Ambient CO<sub>2</sub> in the chamber was monitored periodically and maintained at less than 0.01% by adjusting overall chamber basal ventilation. Humidity was measured and maintained at 40% to 50% by circulating the gas through a freezer and silica gel. Ambient temperature was kept at 22°C to 24°C.

The IH profile consisted of alternating 21.0% and 5.7% O<sub>2</sub> every 180 seconds for the 12-hour light period. Such a profile is associated with reproducible nadir oxyhemoglobin saturations in the 73% to 77% range. Control animals were exposed to circulating room air in 1 of the chambers. Animals were exposed to IH or normoxia for a period of 48 hours and sacrificed immediately after exposure.

### Measurement of Plasma Chemokines

Stromal cell-derived factor-1 (SDF-1), hepatocyte growth factor (HGF), and leukemia inhibitory factor (LIF) levels were measured using commercially available ELISA kits according to the manufacturer's instructions (R&D Systems, Minneapolis, MN). For each exposure condition, i.e., IH and normoxia, 30 independent measurements were performed. For each of these measurements, plasma was pooled from 3 to 4 mice. The SDF-1 assay had a sensitivity of 40 pg/mL and is linear between 100 and 20,000 pg/mL. The interassay and intraassay of coefficients of variability were 3.9% and 7.1%, respectively. The HGF assay had a sensitivity of 55 pg/mL and is linear between 60 and 15,000 pg/mL. The interassay and intraassay of coefficients of variability were 7.7% and 7.1%, respectively. The LIF had a sensitivity of 18 pg/mL and was linear between 20 and 2000 pg/

mL. In our experiments, the interassay and intraassay of coefficients of variability were 6.8% and 4.1%, respectively.

### Statistical Analysis

Comparison of chemokine levels and VSEL counts between IH and normoxia were performed using unpaired, 2-tailed student t-tests, with P values adjusted for unequal variances when appropriate (GraphPad Prism version 5, San Diego CA). Values are reported as mean  $\pm$  standard error of mean (SEM).

### Isolation of VSEL stem cells from BM and PB

VSELs were sorted from a full population of murine BM cells and PB mononuclear cells using multicolor fluorescence-activated cell sorting (FACS), as we have previously described.<sup>26,33</sup> Briefly, mouse BM mononuclear cells were flushed from tibias and femurs, and erythrocytes were removed by a hypotonic solution (Pharm Lyse Buffer; BD Pharmingen, San Jose, CA). Cells were resuspended for staining in medium, containing 2% heat-inactivated FBS (GIBCO). The following rat antimouse antibodies (BD Pharmingen) were employed to detect Sca-1<sup>+</sup> Lin<sup>-</sup> CD45-VSEL-SC: anti-CD45 (APC-Cy7; clone 30-F11), anti-Ly-6A/E (Sca-1) (biotin; clone E13-161.7, with streptavidin conjugated with PE-Cy5), “lineage cocktail”, including anti-CD45R/B220 (PE; clone RA3-6B2), anti-Gr-1 (PE; clone RB6-8C5), anti-TCR  $\alpha$   $\beta$  (PE; clone H57-597), anti-TCR  $\gamma$   $\delta$  (PE; clone GL3), anti-CD11b (PE; clone M1/70), and anti-Ter119 (PE; clone TER-119). Cells were sorted based on size, estimated using bead particles (Flow Cytometry Size Calibration Kit, Invitrogen, Carlsbad, CA) employing MoFlo sorter (DAKO, Carpinteria, CA).

Given the scarcity of VSELs in PB and BM, we performed 6 independent measurements per exposure condition (IH, normoxia), each based on pooled samples from 10 mice (for a total of 120 animals).

### RNA Isolation and Amplification

BM-derived VSELs were isolated from 30 additional mice exposed to IH (pooled into 3 groups of n = 10), and 30 mice were exposed to room air (pooled into 3 groups of n = 10). Total RNA was isolated using PicoPure RNA Isolation Kit (Arcturus Bioscience Inc., Mountain View, CA) following the manufacturer's instructions. RNA amplification was performed using Low-RNA Input Fluorescent Linear Amplification kit (Agilent Technologies, Santa Clara, CA) with modifications. To produce sufficient amount of amplified RNA (cRNA), 2 rounds of RNA amplification were employed using random and T7 primers, respectively, followed by labeling with cyanine 3-dCTP (Cy3-dCTP; Perkin Elmer, Boston, MA).

### Microarray Experiments

For each VSEL-pooled group (n = 10 mice per group), labeled cRNA was hybridized to an Agilent murine whole-genome 60-mer oligo microarray (Agilent Technologies) comprised of more than 45,000 probes. Six independent hybridizations (3 pooled samples from mice exposed to IH and 3 pooled samples from normoxic mice) were performed. Microarrays were scanned using SureScan technology and images processed with Feature Extraction 9.5 software (Agilent Technologies). Background-subtracted intensities were normalized across all microarrays using the quantile method.<sup>36</sup>

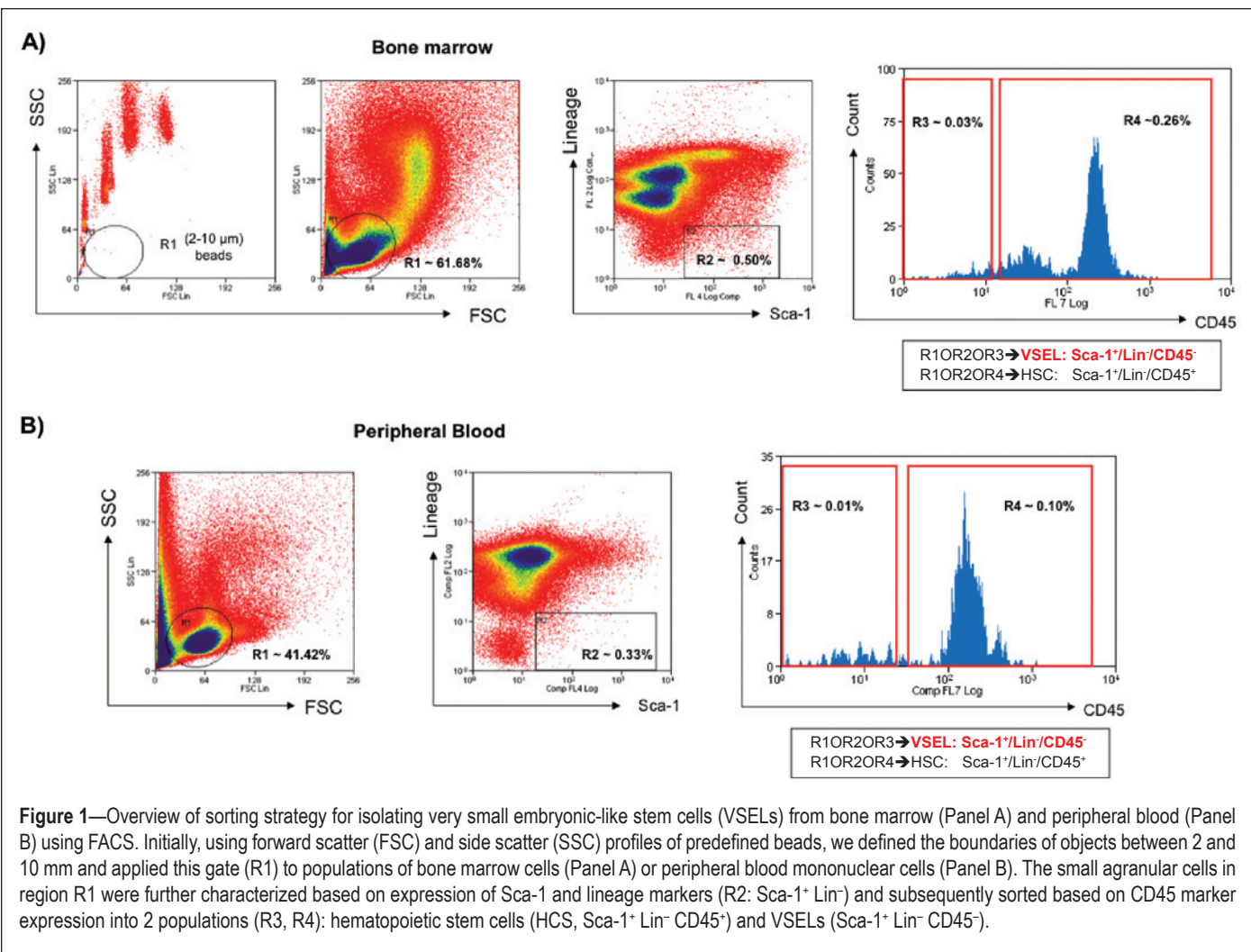


**Figure 1**—Overview of sorting strategy for isolating very small embryonic-like stem cells (VSELs) from bone marrow (Panel A) and peripheral blood (Panel B) using FACS. Initially, using forward scatter (FSC) and side scatter (SSC) profiles of predefined beads, we defined the boundaries of objects between 2 and 10 mm and applied this gate (R1) to populations of bone marrow cells (Panel A) or peripheral blood mononuclear cells (Panel B). The small agranular cells in region R1 were further characterized based on expression of Sca-1 and lineage markers (R2: Sca-1<sup>+</sup> Lin<sup>-</sup>) and subsequently sorted based on CD45 marker expression into 2 populations (R3, R4): hematopoietic stem cells (HCS, Sca-1<sup>+</sup> Lin<sup>-</sup> CD45<sup>+</sup>) and VSELs (Sca-1<sup>+</sup> Lin<sup>-</sup> CD45<sup>-</sup>).

## Gene-Expression Analysis

Multidimensional scaling using principal components analysis (PCA) was performed based on the covariance matrix of approximately 45,000 normalized gene-expression values.<sup>37</sup> Differential gene expression in VSELs exposed to IH versus normoxia was determined using a Bayesian implementation of the parametric t-test designed for robust analysis of microarray experiments with modest replicates.<sup>38</sup> Multiple-hypothesis testing was addressed by false discovery rate (FDR) analysis using the Q-value<sup>39</sup> method. A cutoff Q value of less than 0.05 was used for significant differential gene expression.

## Functional Pathway and Network Analyses

Differentially expressed genes in VSELs (Q value < 0.05) underwent Gene Ontology analysis using the Database for Annotation, Visualization and Integrated Discovery (DAVID) program.<sup>40</sup> Enrichment of functional processes was determined using P values derived from a modified Fisher exact test. Functional annotation clustering of enriched categories was used to identify and group biologic modules with similar gene members based on the  $\kappa$  coefficient.<sup>40</sup> A permutation-based FDR analysis was employed to correct for multiple-hypothesis testing (FDR cutoff < 5%).

We then constructed a gene product interaction network of differentially expressed genes in VSELs during exposure to IH

based on previously published direct and indirect interactions using Ingenuity knowledge base<sup>41</sup> and several publicly available databases. The topologic characteristic of the resulting network was studied by using its connectivity matrix. To assess whether the network possessed “scale-free” properties, i.e., followed a power-law distribution, the degree distribution of its nodes,  $N_k$ , was plotted against the connectivity of the nodes,  $k$ .<sup>42</sup> Next, we extracted a subnetwork from the original network, and limited the subnetwork to nodes involved in developmental processes, as determined by our Gene Ontology analysis.

## RESULTS

### VSELs Can Be Isolated and Quantified from Murine BM and PB

Employing a systematic gating strategy using FACS, based on size, granularity, and specific antibody staining, we isolated rare populations of VSELs from PB and BM of mice exposed to normoxia and IH (Figure 1).

### Exposure to IH Mobilizes VSELs from the BM into PB

Isolation of VSELs from BM and PB of mice exposed to either normoxia or IH revealed a significant increase in the peripheral count of these pluripotent stem cells during IH (Figure 2A) and a concomitant reduction in the BM reserve pool (Figure 2B). The relative effect of IH in mobilizing VSELs

from BM to PB in response to IH is shown in Figure 2C. Furthermore, IH was associated with a significant increase in plasma levels of the stem cell chemoattractants SDF-1, HGF, and LIF (Figure 2D-F), providing further evidence that exposure to IH promotes a favorable gradient for recruitment of VSELs from BM to PB.

### Exposure to IH Induces a Distinct Transcriptional Response in VSELs

Differential variability in genome-wide expression profiles of BM-derived VSELs exposed to IH and normoxia was assessed using PCA. This analysis robustly segregated the 2 exposure groups (Figure 3), implying that IH causes a global perturbation in the VSEL transcriptome. We then statistically identified

1113 differentially expressed genes in VSELs exposed to IH versus normoxia at a Q-value cutoff of less than 0.05. (See supplementary section, Table S1. Supplementary material is available online only at [www.journalsleep.org](http://www.journalsleep.org).) These differentially expressed genes underwent further computational analyses as described below.

### IH Activates Organ-Specific Developmental Programs in VSELs

To determine whether genes differentially expressed during IH map to coherent biologic processes, we performed Gene Ontology analysis followed by functional annotation clustering.<sup>40</sup> The most significant functional cluster was “multicellular organismal development” (enrichment P value  $9.7 \times 10^{-11}$ , FDR  $1.7 \times 10^{-11}$ ), but several other developmental processes were also highly overrepresented, including those involved in angiogenesis, central nervous system (CNS) development, and tube/lung development (supplementary section, Table S2). Figure 4 depicts a wiring-diagram representation of these enriched developmental modules and highlights the intermodular connections resulting from the genes that are shared among them. These findings demonstrate that a brief exposure to IH induces a transcriptional response in BM-derived VSELs that is highly enriched in multi-organ developmental programs.

### Network Analysis of VSEL Transcriptome Reveals the Interaction of Key Developmental Regulators During IH

Because biologic processes are often orchestrated by co-regulated changes among many genes, we created a gene product interaction network, or interactome, of IH-induced differentially expressed genes in VSELs (Figure 5A). This network consisted of 387 genes (nodes) and 620 connections (edges). Topologic analysis of this interactome demonstrated that, consistent with many biologic networks, it is scale free and follows a power law distribution—i.e.,  $N_k \sim k^{-\gamma}$  ( $\gamma = 1.39$ ,  $R^2 = 0.98$ )

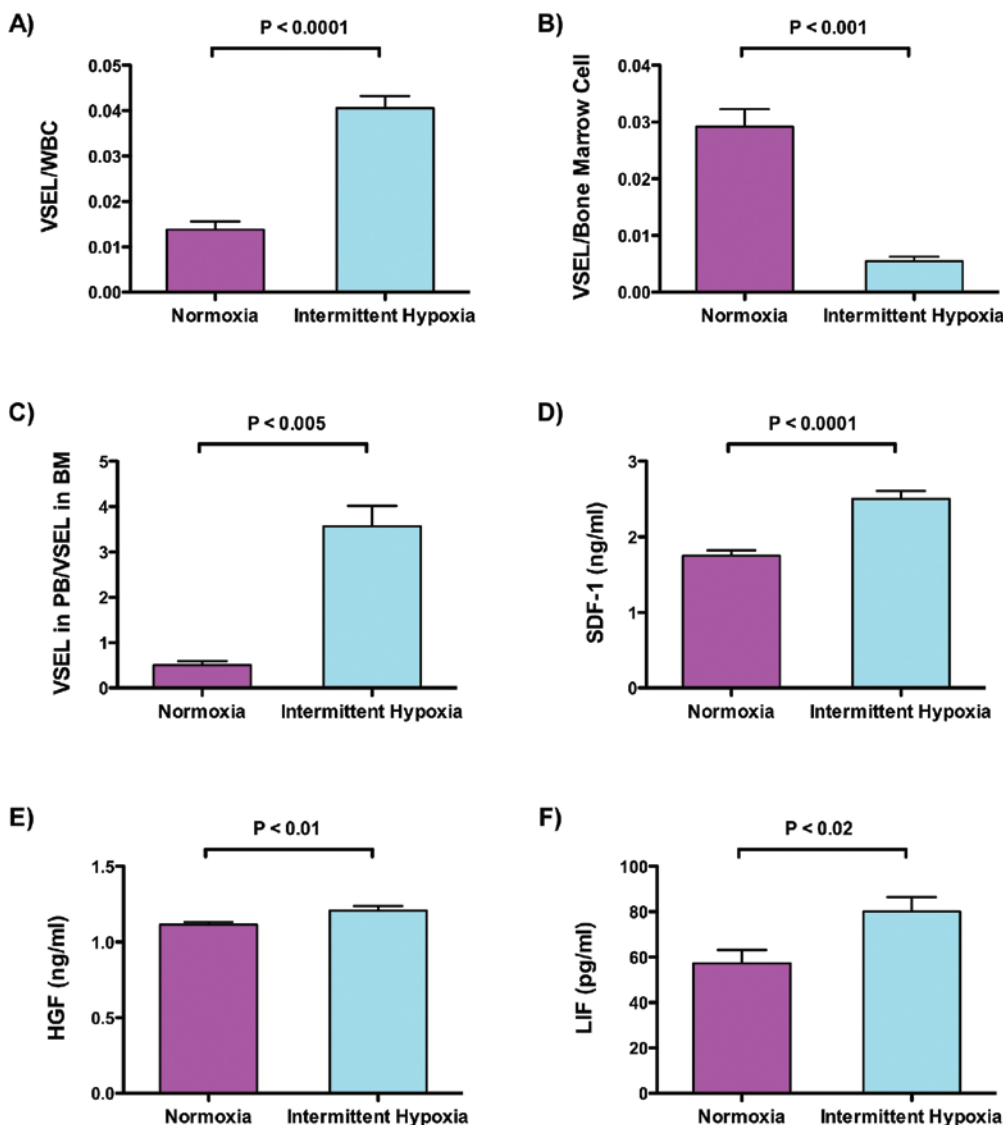


**Figure 2**—Mobilization of very small embryonic-like stem cells (VSEL) from bone marrow (BM) to peripheral blood (PB) and development of chemokine gradients in plasma after exposure to intermittent hypoxia profile for 48 hours. Panels A-C demonstrate significant increases in PB counts of VSEL (normalized for total leukocyte numbers) and concomitant decrease in the relative ratio of these stem cells in BM. Panels D-F show significant elevation in protein levels of 3 stem cell chemoattractants in response to intermittent hypoxia: stromal cell-derived factor-1 (SDF-1), hepatocyte growth factor (HGF), and leukemia inhibitory factor (LIF). The values displayed are means  $\pm$  standard error of mean (SEM). P values were calculated using unpaired student t-test.

where  $N_k$  is the degree distribution and  $k$  is the nodal connectivity (Figure 5B). Network nodes mapping to the “development module” are highlighted in a darker shade, confirming that this functional module comprises a significant proportion of the membership of the interactome. To better evaluate the links among members of this highly enriched module, we extracted a subnetwork limited to these genes (Figure 6). This “developmental interactome” captures the complex relationships among genes mapping to the “development module” in Figure 4. Members of the network involved in CNS, blood vessel, or tube/lung development are highlighted in different colors for illustration purposes. A select number of representative nodes regulating these processes are labeled in Figure 6, including vascular endothelial growth factor receptor-1 (*Flt1*), angiopoietin-1 (*Angpt1*), epidermal growth factor (*Egf*), peroxisome proliferator activated receptor- $\gamma$  (*Pparg*), glucose transporter type-4 (*Glut4*), stromal cell-derived factor-1 (*Sdf1*), dishevelled-1 (*Dvl1*), and vang-like 1 and 2 (*Vangl1*, *Vangl2*). A fully labeled network is available in the supplementary section (Figure S1).

## DISCUSSION

In this study, we show that exposure to IH during the circadian rest period (i.e., daylight hours) promotes induction of distinct stem cell chemoattractant gradients in PB of mice and robustly mobilizes pluripotent VSELs from BM to the peripheral circulation. Since IH is a key pathophysiologic feature of OSA, our findings raise the possibility that this phenomenon also occurs in the clinical setting. Recent studies by Carreras et al. showed that mesenchymal stem cells are released into the peripheral circulation of anesthetized rats exposed to recurrent apneas for 6 hours<sup>43</sup> and that injection of mesenchymal stem cells can reduce markers of inflammation.<sup>44</sup> Despite similar findings, there are important differences between our approaches. Firstly, we studied different stem cell populations. VSELs are very rare pluripotent cells occupying the highest level in

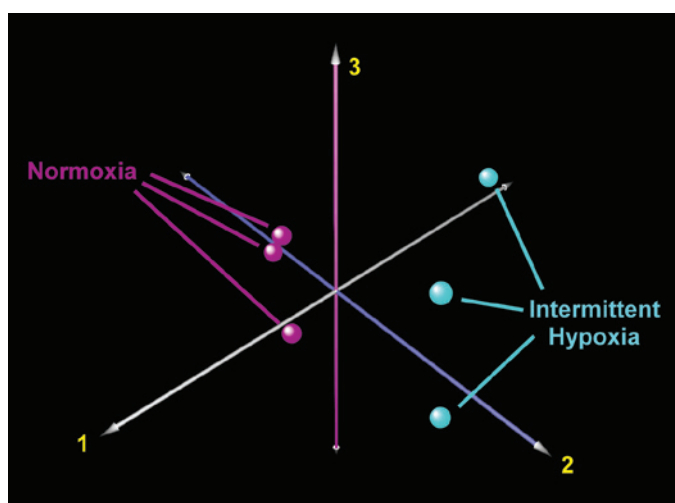


**Figure 3**—Principal component analysis of bone marrow-derived very small embryonic-like stem cells (VSELs) gene expression from mice exposed to intermittent hypoxia and normoxia. The clear segregation and prominent clustering of the experiments into 2 groups implies that exposure to intermittent hypoxia elicits a distinct genome-wide transcriptional perturbation in these pluripotent stem cells.

the hierarchical organization of stem cells because they can self renew and differentiate into all 3 germ layers, whereas mesenchymal stem cells represent a more populous and lineage-committed stem cell pool that differentiate only into mesenchymal tissues, such as bone, adipose tissue, and muscle. Secondly, our experimental exposure to IH occurred during the natural sleep cycle of mice and without instrumentation or anesthesia. Notwithstanding, the consistency between our findings supports the proposition that recurrent hypoxia promotes recruitment of various stem cell populations from the BM into the PB and that such recruitment should be apparent in patients with OSA as well. Indeed, we and others have shown that OSA is associated with alterations in the levels of circulating endothelial progenitor cells in adult<sup>45</sup> and pediatric<sup>46</sup> populations, thereby further lending support to the notion that OSA and/or IH will not only activate organ injury-related processes, but also recruit repair mechanisms that may mitigate the magnitude of morbidity or facilitate recovery upon treatment and cessation of IH.

Although we found that VSELs were activated and mobilized during in vivo exposure to IH, the genetic programs orchestrating this response remained unexplored. We therefore proceeded to systematically explore the transcriptional consequences of IH on these unique rare clusters of pluripotent stem cells using expression profiling followed by functional and network analysis. Initial analysis revealed that exposure to IH induces a distinct global transcriptional signature in VSELs. More than 1000 unique genes were differentially expressed in BM-derived VSELs in response to IH, and their interacting network possessed scale-free properties characteristic of complex biologic networks.<sup>47,48</sup> Importantly, functional analysis of the differentially expressed genes revealed that multiple, organ-specific developmental programs were enriched during IH exposure (Figure 4). Consistent with the pluripotent embryonic-like properties of VSELs, these modules encompassed developmental processes originating from the differentiation of distinct germ lines, including ectoderm (CNS CNS development), me-

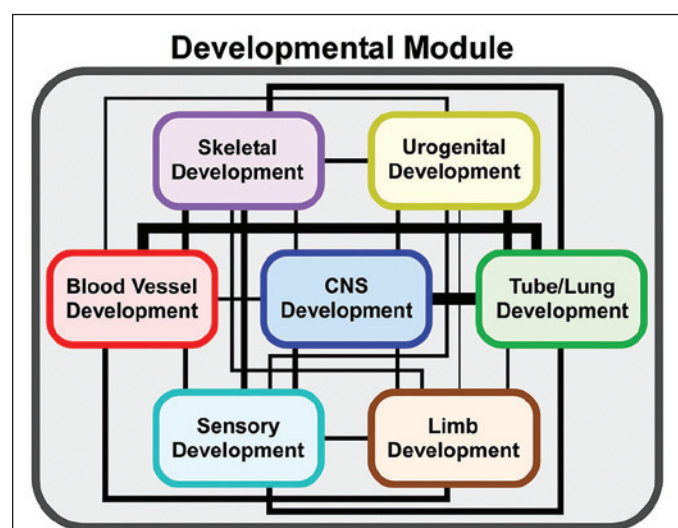
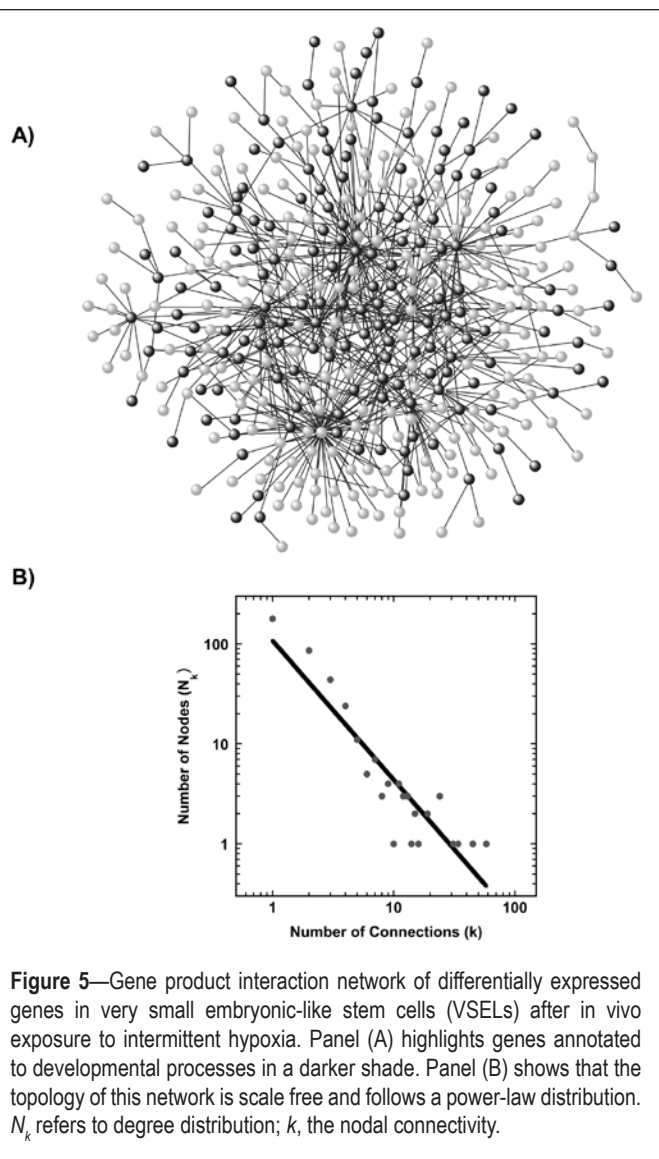
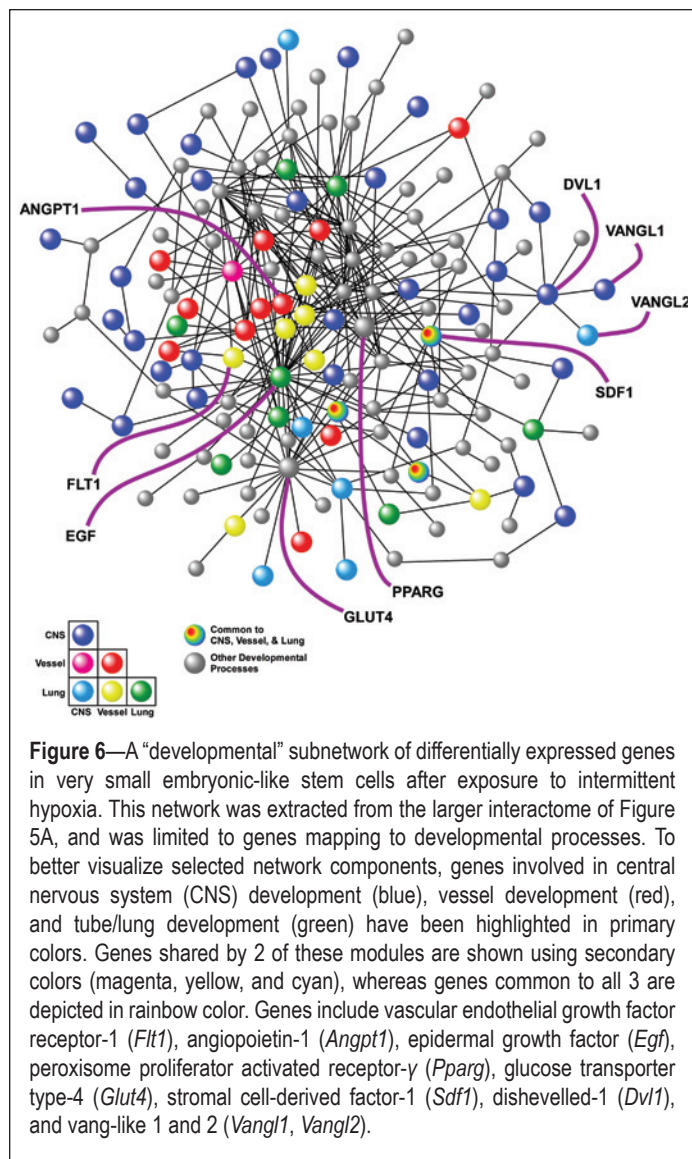


**Figure 4**—Enriched biologic processes involved in specific organ development are depicted using a wiring diagram. The intermodular connections reflect the fact that some genes map to multiple modules, whereas the line thickness is proportional to the number of shared genes. CNS refers to central nervous system.



soderm (blood vessel and skeletal development), and endoderm (tube/lung development).

To further understand the gene-product relationships within the highly enriched developmental module, we extracted a genetic interaction network from the large network of differentially expressed genes (Figure 6). This analysis attributed functional roles for specific differentially expressed candidate genes. It was reassuring to find among such highly enriched genes within this interactome—the stem cell chemoattractant *Sdf1*, which also mapped to multiple developmental processes. Other members of this developmental network included vascular *Flt1* and *Angptl*—2 critical regulators of angiogenesis.<sup>49,50</sup> The most densely connected node within the network was *Egf*, a controller of branching morphogenesis<sup>51</sup> and a key ligand in the EGFR signaling cascade regulating many developmental, proliferative, and transformative processes.<sup>52</sup> Several interacting gene products—including *Dvl1*, *Vangl1*, and *Vangl2*—were members of the CNS development module. Mutations in *Vangl1* and *Vangl2* have been linked to neural-tube defects in mice<sup>53</sup> and humans,<sup>54</sup> whereas *Dvl1* functionally interacts with these genes during CNS development.<sup>55</sup> Interestingly, transgenic mice lacking *Dvl1* exhibit abnormality in their social behavior, sensorimotor gat-



ing, and sleep patterns.<sup>56</sup> A number of the nodes (shown in gray, Figure 6) did not map to enriched developmental submodules (as depicted in Figure 4) but were, nevertheless, members of the developmental network. Prominent examples included *Pparg* and *Glut4*. The products of these genes play critical roles in adipogenesis<sup>57</sup> and maintenance of glucose homeostasis.<sup>58</sup>

Taken together, these results imply that *in vivo* exposure to IH activates distinct and selective transcriptional programs in BM-derived pluripotent stem cells. Intriguingly, many of these differentially enriched developmental processes map to organs or pathways known to be adversely affected in OSA, including the CNS, vascular system, and metabolism.<sup>59</sup> This finding raises the possibility that, in response to IH, VSELs activate regenerative programs tailored for end organs that are either injured or at increased risk for injury.

Our study has a number of limitations. The murine model of IH does not capture the pathophysiologic complexity of OSA, since it does not incorporate sleep fragmentation, recurrent hypercapnia, and increased intrathoracic pressure swings. Furthermore, we have restricted our studies to the effects of short-term exposure to IH—chronic exposure to IH, as seen in OSA, may result in different patterns of VSEL recruitment

and the activation of different transcriptional programs. Our animal-based findings may not be generalizable to humans, although previous studies on VSEL recruitment during stroke and myocardial infarction reported similar responses in humans<sup>35,60</sup> and in mice.<sup>27,30</sup> Our functional and network analysis of the VSEL transcriptome is limited by the current state of knowledge and can yield different results in future iterations. Additionally, components of this interactome may represent a generalized response of VSELs to other pathophysiologic perturbations and, therefore, may not be specific to IH exposures. Although compelling, our results do not unequivocally prove that recruited VSELs in PB originated from the BM, since it is possible that some of these stem cells were mobilized from other tissue depots. However, BM is the predominant repository of VSELs and likely the primary source of the increased numbers observed during IH in PB. Finally, we have not demonstrated that mobilized populations of BM-derived VSELs are recruited to specific target organs in response to IH, where they undergo lineage differentiation and proliferation. Further studies are clearly required to elucidate the fate of these IH-activated pluripotent stem cells in circulating blood and to investigate their role within specific tissue compartments.

In summary, we report that exposure to IH during sleep for 48 hours alters stem cell chemoattractant gradients in plasma and mobilizes VSELs from BM to the peripheral circulation. A systematic analysis of the VSEL transcriptome further reveals selective activation of developmental programs in response to IH, including those involved in CNS development and angiogenesis. Future work is needed to establish the regenerative mechanisms initiated by these transcriptional programs upon recruitment of pluripotent stem cells to at-risk organs.

## ACKNOWLEDGMENTS

This work was supported in part by the National Institutes of Health HL065270 and HL086662 (DG), and American Sleep Medicine Foundation Junior Faculty Research Award (SAG).

## DISCLOSURE STATEMENT

This was not an industry supported study. Dr. Gozal has participated in speaking engagements for Merck and has consulted for Galleon Pharmaceuticals. The other authors have indicated no financial conflicts of interest.

## REFERENCES

- Lumeng JC, Chervin RD. Epidemiology of pediatric obstructive sleep apnea. *Proc Am Thorac Soc* 2008;5:242-52.
- Punjabi NM. The epidemiology of adult obstructive sleep apnea. *Proc Am Thorac Soc* 2008;5:136-43.
- Young T, Palta M, Dempsey J, Skatrud J, Weber S, Badr S. The occurrence of sleep-disordered breathing among middle-aged adults. *N Engl J Med* 1993;328:1230-5.
- Park AM, Suzuki YJ. Effects of intermittent hypoxia on oxidative stress-induced myocardial damage in mice. *J Appl Physiol* 2007;102:1806-14.
- Punjabi NM, Sorkin JD, Katzel LI, Goldberg AP, Schwartz AR, Smith PL. Sleep-disordered breathing and insulin resistance in middle-aged and overweight men. *Am J Respir Crit Care Med* 2002;165:677-82.
- Young T, Peppard PE, Gottlieb DJ. Epidemiology of obstructive sleep apnea: a population health perspective. *Am J Respir Crit Care Med* 2002;165:1217-39.
- Hirshkowitz M. The clinical consequences of obstructive sleep apnea and associated excessive sleepiness. *J Fam Pract* 2008;57:S9-16.
- Nieto FJ, Young TB, Lind BK, et al. Association of sleep-disordered breathing, sleep apnea, and hypertension in a large community-based study. *Sleep Heart Health Study. JAMA* 2000;283:1829-36.
- Redline S, Strohl KP. Recognition and consequences of obstructive sleep apnea hypopnea syndrome. *Clin Chest Med* 1998;19:1-19.
- Strohl KP. Diabetes and sleep apnea. *Sleep* 1996;19:S225-8.
- Minoguchi K, Yokoe T, Tazaki T, et al. Silent brain infarction and platelet activation in obstructive sleep apnea. *Am J Respir Crit Care Med* 2007;175:612-7.
- Alchanatis M, Deligiorgis N, Zias N, et al. Frontal brain lobe impairment in obstructive sleep apnoea: a proton MR spectroscopy study. *Eur Respir J* 2004;24:980-6.
- Beebe DW, Gozal D. Obstructive sleep apnea and the prefrontal cortex: towards a comprehensive model linking nocturnal upper airway obstruction to daytime cognitive and behavioral deficits. *J Sleep Res* 2002;11:1-16.
- Morrell MJ, McRobbie DW, Quest RA, Cummin AR, Ghiasi R, Corfield DR. Changes in brain morphology associated with obstructive sleep apnea. *Sleep Med* 2003;4:451-4.
- Gozal D. Sleep-disordered breathing and school performance in children. *Pediatrics* 1998;102:616-20.
- Polotsky VY, O'Donnell CP. Genomics of sleep-disordered breathing. *Proc Am Thorac Soc* 2007;4:121-6.
- Gozal D, Daniel JM, Dohanich GP. Behavioral and anatomical correlates of chronic episodic hypoxia during sleep in the rat. *J Neurosci* 2001;21:2442-50.
- Iiyori N, Alonso LC, Li J, et al. Intermittent hypoxia causes insulin resistance in lean mice independent of autonomic activity. *Am J Respir Crit Care Med* 2007;175:851-7.
- Row BW, Kheirandish L, Li RC, et al. Platelet-activating factor receptor-deficient mice are protected from experimental sleep apnea-induced learning deficits. *J Neurochem* 2004;89:189-96.
- Row BW, Liu R, Xu W, Kheirandish L, Gozal D. Intermittent hypoxia is associated with oxidative stress and spatial learning deficits in the rat. *Am J Respir Crit Care Med* 2003;167:1548-53.
- Reeves SR, Gozal E, Guo SZ, et al. Effect of long-term intermittent and sustained hypoxia on hypoxic ventilatory and metabolic responses in the adult rat. *J Appl Physiol* 2003;95:1767-74.
- Zhan G, Serrano F, Fenik P, et al. NADPH oxidase mediates hypersomnolence and brain oxidative injury in a murine model of sleep apnea. *Am J Respir Crit Care Med* 2005;172:921-9.
- Reeves SR, Gozal D. Platelet-activating factor receptor modulates respiratory adaptation to long-term intermittent hypoxia in mice. *Am J Physiol Regul Integr Comp Physiol* 2004;287:R369-74.
- Tagaito Y, Polotsky VY, Campen MJ, et al. A model of sleep-disordered breathing in the C57BL/6J mouse. *J Appl Physiol* 2001;91:2758-66.
- Reeves SR, Gozal D. Platelet-activating factor receptor and respiratory and metabolic responses to hypoxia and hypercapnia. *Respir Physiol Neurobiol* 2004;141:13-20.
- Kucia MJ, Wysoczynski M, Wu W, Zuba-Surma EK, Ratajczak J, Ratajczak MZ. Evidence that very small embryonic-like stem cells are mobilized into peripheral blood. *Stem Cells* 2008;26:2083-92.
- Zuba-Surma EK, Kucia M, Dawn B, Guo Y, Ratajczak MZ, Bolli R. Bone marrow-derived pluripotent very small embryonic-like stem cells (VSELs) are mobilized after acute myocardial infarction. *J Mol Cell Cardiol* 2008;44:865-73.
- Abbott JD, Huang Y, Liu D, Hickey R, Krause DS, Giordano FJ. Stromal cell-derived factor-1alpha plays a critical role in stem cell recruitment to the heart after myocardial infarction but is not sufficient to induce homing in the absence of injury. *Circulation* 2004;110:3300-5.
- Kucia M, Dawn B, Hunt G, et al. Cells expressing early cardiac markers reside in the bone marrow and are mobilized into the peripheral blood after myocardial infarction. *Circ Res* 2004;95:1191-9.
- Kucia M, Zhang YP, Reca R, et al. Cells enriched in markers of neural tissue-committed stem cells reside in the bone marrow and are mobilized into the peripheral blood following stroke. *Leukemia* 2006;20:18-28.
- Schachinger V, Erbs S, Elsasser A, et al. Intracoronary bone marrow-derived progenitor cells in acute myocardial infarction. *N Engl J Med* 2006;355:1210-21.

32. Tendera M, Wojakowski W, Ruzylo W, et al. Intracoronary infusion of bone marrow-derived selected CD34+CXCR4+ cells and non-selected mononuclear cells in patients with acute STEMI and reduced left ventricular ejection fraction: results of randomized, multicentre Myocardial Regeneration by Intracoronary Infusion of Selected Population of Stem Cells in Acute Myocardial Infarction (REGENT) Trial. *Eur Heart J* 2009;30:1313-21.
33. Kucia M, Reca R, Campbell FR, et al. A population of very small embryonic-like (VSEL) CXCR4(+)SSEA-1(+)Oct-4+ stem cells identified in adult bone marrow. *Leukemia* 2006;20:857-69.
34. Kucia M, Wojakowski W, Reca R, et al. The migration of bone marrow-derived non-hematopoietic tissue-committed stem cells is regulated in an SDF-1-, HGF-, and LIF-dependent manner. *Arch Immunol Ther Exp (Warsz)* 2006;54:121-35.
35. Paczkowska E, Kucia M, Koziarska D, et al. Clinical evidence that very small embryonic-like stem cells are mobilized into peripheral blood in patients after stroke. *Stroke* 2009;40:1237-44.
36. Bolstad BM, Irizarry RA, Astrand M, Speed TP. A comparison of normalization methods for high density oligonucleotide array data based on variance and bias. *Bioinformatics* 2003;19:185-93.
37. Saeed AI, Sharov V, White J, et al. TM4: a free, open-source system for microarray data management and analysis. *Biotechniques* 2003;34:374-8.
38. Baldi P, Long AD. A Bayesian framework for the analysis of microarray expression data: regularized t -test and statistical inferences of gene changes. *Bioinformatics* 2001;17:509-19.
39. Storey JD, Tibshirani R. Statistical significance for genomewide studies. *Proc Natl Acad Sci U S A* 2003;100:9440-5.
40. Dennis G, Jr., Sherman BT, Hosack DA, et al. DAVID: Database for Annotation, Visualization, and Integrated Discovery. *Genome Biol* 2003;4:P3.
41. Calvano SE, Xiao W, Richards DR, et al. A network-based analysis of systemic inflammation in humans. *Nature* 2005;437:1032-7.
42. Barabasi AL, Albert R. Emergence of scaling in random networks. *Science* 1999;286:509-12.
43. Carreras A, Almendros I, Acerbi I, Montserrat JM, Navajas D, Farre R. Obstructive apneas induce early release of mesenchymal stem cells into circulating blood. *Sleep* 2009;32:117-9.
44. Carreras A, Almendros I, Montserrat JM, Navajas D, Farre R. Mesenchymal stem cells reduce inflammation in a rat model of obstructive sleep apnea. *Respir Physiol Neurobiol* 2010 (in press).
45. Jelic S, Padeletti M, Kawut SM, et al. Inflammation, oxidative stress, and repair capacity of the vascular endothelium in obstructive sleep apnea. *Circulation* 2008;117:2270-8.
46. Kheirandish-Gozal L, Bhattacharjee R, Kim J, Clair HB, Gozal D. Endothelial Progenitor Cells and Vascular Dysfunction in Children with Obstructive Sleep Apnea. *Am J Respir Crit Care Med* 2010;182:92-7.
47. Barabasi AL, Oltvai ZN. Network biology: understanding the cell's functional organization. *Nat Rev Genet* 2004;5:101-13.
48. Khalifa A, Gharib SA, Kim J, et al. Transcriptomic analysis identifies phosphatases as novel targets for adenotonsillar hypertrophy of pediatric obstructive sleep apnea. *Am J Respir Crit Care Med* 2010;181:1114-20.
49. Augustin HG, Koh GY, Thurston G, Alitalo K. Control of vascular morphogenesis and homeostasis through the angiopoietin-Tie system. *Nat Rev Mol Cell Biol* 2009;10:165-77.
50. Adams RH, Alitalo K. Molecular regulation of angiogenesis and lymphangiogenesis. *Nat Rev Mol Cell Biol* 2007;8:464-78.
51. Cardoso WV. Molecular regulation of lung development. *Annu Rev Physiol* 2001;63:471-94.
52. Oda K, Matsuka Y, Funahashi A, Kitano H. A comprehensive pathway map of epidermal growth factor receptor signaling. *Mol Syst Biol* 2005;1:2005 0010.
53. Torban E, Patenaude AM, Leclerc S, et al. Genetic interaction between members of the Vangl family causes neural tube defects in mice. *Proc Natl Acad Sci U S A* 2008;105:3449-54.
54. Kibar Z, Torban E, McDermid JR, et al. Mutations in VANGL1 associated with neural-tube defects. *N Engl J Med* 2007;356:1432-7.
55. Torban E, Wang HJ, Groulx N, Gros P. Independent mutations in mouse Vangl2 that cause neural tube defects in looptail mice impair interaction with members of the Dishevelled family. *J Biol Chem* 2004;279:52703-13.
56. Lijam N, Paylor R, McDonald MP, et al. Social interaction and sensorimotor gating abnormalities in mice lacking Dvl1. *Cell* 1997;90:895-905.
57. Rosen ED, Sarraf P, Troy AE, et al. PPAR gamma is required for the differentiation of adipose tissue in vivo and in vitro. *Mol Cell* 1999;4:611-7.
58. Huang S, Czech MP. The GLUT4 glucose transporter. *Cell Metab* 2007;5:237-52.
59. Dempsey JA, Veasey SC, Morgan BJ, O'Donnell CP. Pathophysiology of sleep apnea. *Physiol Rev* 2010;90:47-112.
60. Wojakowski W, Tendera M, Michalowska A, et al. Mobilization of CD34/CXCR4+, CD34/CD117+, c-met+ stem cells, and mononuclear cells expressing early cardiac, muscle, and endothelial markers into peripheral blood in patients with acute myocardial infarction. *Circulation* 2004;110:3213-20.

Table S1

## Differentially Expressed Genes in Bone Marrow-derived VSELs Exposed to Intermittent Hypoxia

Gene Symbol	Entrez ID	P-value	Q-value	Log <sub>2</sub> [IH/Normoxia]	Description
Abl2	11352	2.35E-03	4.30E-02	-1.871	v-abl Abelson murine leukemia viral oncogene homolog 2 (arg, Abelson-related gene) (Abl2), transcript variant 2, 8 days embryo whole body cDNA, RIKEN full-length enriched library, clone:5730407E21 product:acid phosphatase, acrosin prepropeptide (Acr), mRNA [NM_013455]
Acp2	11432	3.51E-04	1.14E-02	-1.619	adiponectin, C1Q and collagen domain containing (Adipoq), mRNA [NM_009605]
Acr	11434	1.32E-04	5.66E-03	1.838	actin, beta (Actb), mRNA [NM_007393]
Adipoq	11450	4.54E-06	4.01E-04	1.580	a disintegrin-like and metalloproteinase (reprolysin type) with thrombospondin type 1 motif, 1 (Adamts1), mRNA [NM_007409]
Actb	11461	1.46E-04	6.19E-03	1.965	alcohol dehydrogenase 1 (class I) (Adh1), mRNA [NM_007409]
Adamts1	11504	9.10E-06	6.92E-04	1.698	G protein-coupled receptor 182 (Gpr182), mRNA [NM_007412]
Adh1	11522	3.65E-06	3.42E-04	1.782	alpha fetoprotein (Afp), mRNA [NM_007423]
Gpr182	11536	1.52E-05	1.05E-03	1.374	advanced glycosylation end product-specific receptor (Ager), mRNA [NM_007425]
Afp	11576	3.35E-04	1.10E-02	-1.719	angiopoietin 1 (Angpt1), mRNA [NM_009640]
Ager	11596	2.40E-03	4.36E-02	-1.629	alpha-2-HS-glycoprotein (Ahsg), mRNA [NM_013465]
Angpt1	11600	6.11E-07	8.05E-05	-2.230	Alas1
Ahsg	11625	1.18E-03	2.74E-02	-3.153	aminolevulinic acid synthase 1 (Alas1), mRNA [NM_020559]
Alas1	11655	1.57E-03	3.27E-02	0.694	Alas2
Alas2	11656	1.49E-07	2.64E-05	2.046	aminolevulinic acid synthase 2, erythroid (Alas2), nuclear gene encoding mitochondrial protein, transcript variant adult male corpora quadrigemina cDNA, RIKEN full-length enriched library, clone:B230105J09 product:aldehyde reductase (Alrd)
Aldh2	11669	5.51E-04	1.55E-02	1.176	Prdx6
Prdx6	11758	1.21E-05	8.68E-04	-2.813	Fabp4
Fabp4	11770	7.54E-09	2.16E-06	1.732	Apb2b
Apb2b	11787	3.98E-04	1.25E-02	1.303	Speg
Speg	11790	3.18E-05	1.90E-03	3.353	Apoc1
Apoc1	11812	1.50E-03	3.17E-02	1.289	apolipoprotein C-I (Apoc1), transcript variant 1, mRNA [NM_007469]
Apoe	11816	2.81E-05	1.72E-03	0.974	apolipoprotein E (Apoe), mRNA [NM_009696]
Aqr	11834	2.46E-14	9.89E-11	-3.830	Rplp0
Rplp0	11837	3.65E-05	2.10E-03	1.089	Rhoc
Rhoc	11853	2.73E-04	9.69E-03	0.905	Arvcf
Arvcf	11877	2.09E-03	3.95E-02	-2.058	Atm
Atm	11920	1.53E-05	1.05E-03	-2.259	Barx2
Barx2	12023	1.53E-05	1.05E-03	-2.655	Bcl2l11
Bcl2l11	12125	9.29E-04	2.27E-02	1.281	Fabp7
Fabp7	12140	6.01E-04	1.64E-02	-6.486	Bnip3l
Bnip3l	12177	2.28E-03	4.20E-02	0.696	Serp1
Serp1	12258	1.14E-03	2.65E-02	1.286	C4b
C4b	12268	9.36E-04	2.28E-02	1.723	Calb1
Calb1	12307	2.80E-10	1.53E-07	-2.589	Aspm
Aspm	12316	8.23E-05	3.98E-03	-1.835	Camk4
Camk4	12326	9.78E-06	7.39E-04	4.137	Car2
Car2	12349	9.18E-04	2.25E-02	0.732	Casp12
Casp12	12364	6.76E-04	1.79E-02	3.049	Casp3
Casp3	12367	1.42E-03	3.07E-02	-2.188	Cbni1
Cbni1	12404	4.42E-07	6.20E-05	3.306	Serpinh1
Serpinh1	12406	1.06E-05	7.82E-04	1.746	Cbx2
Cbx2	12416	6.75E-06	5.49E-04	-2.744	Cd36
Cd36	12491	7.53E-04	1.94E-02	1.305	Cd48
Cd48	12506	3.93E-06	3.59E-04	-2.467	Cd72
Cd72	12517	5.66E-04	1.58E-02	-1.175	Cdgap
Cdgap	12549	1.14E-03	2.65E-02	1.294	Cdh5
Cdh5	12562	1.95E-04	7.71E-03	1.511	Cdkn2b
Cdkn2b	12579	2.83E-05	1.72E-03	-2.146	Cenpb
Cenpb	12616	3.07E-04	1.05E-02	-3.449	Ch25h
Ch25h	12642	8.91E-07	1.09E-04	-3.542	Chd1
Chd1	12648	6.89E-04	1.81E-02	-1.067	Cica1
Cica1	12722	7.38E-06	5.83E-04	1.618	Cldn5
Cldn5	12741	1.27E-05	8.98E-04	1.468	Il8rb
Il8rb	12765	3.85E-04	1.22E-02	-1.195	Cxcr7
Cxcr7	12778	8.57E-08	1.67E-05	3.817	Cnn1
Cnn1	12797	1.47E-03	3.13E-02	-1.789	Col11a1
Col11a1	12814	1.95E-06	2.10E-04	3.616	Col3a1
Col3a1	12825	3.38E-06	3.23E-04	2.364	Col4a1
Col4a1	12826	4.83E-05	2.65E-03	1.818	Col4a2
Col4a2	12827	2.51E-03	4.53E-02	1.984	Col8a1
Col8a1	12837	5.66E-05	2.95E-03	1.883	Col1a2
Col1a2	12843	1.93E-03	3.75E-02	0.932	Cox6a2
Cox6a2	12862	4.08E-04	1.27E-02	-0.861	Cp
Cp	12870	3.91E-04	1.24E-02	1.680	Cpne6
Cpne6	12891	8.23E-04	2.09E-02	1.629	Bcar1
Bcar1	12927	1.48E-03	3.15E-02	1.084	Dmbt1
Dmbt1	12945	2.84E-04	9.92E-03	2.165	Crym
Crym	12971	1.31E-03	2.93E-02	2.656	Csf1r
Csf1r	12978	1.65E-03	3.37E-02	-1.269	Csf2
Csf2	12981	2.72E-04	9.69E-03	-1.824	Cux1
Cux1	13047	1.16E-06	1.36E-04	-2.880	Cyb561
Cyb561	13056	3.17E-04	1.06E-02	2.061	Cyp4b1
Cyp4b1	13120	1.56E-06	1.75E-04	2.344	Dab2
Dab2	13132	1.05E-05	7.79E-04	1.624	Dck
Dck	13178	2.79E-12	3.06E-09	-3.207	Dcn
Dcn	13179	6.57E-13	1.16E-09	3.939	Des
Des	13346	3.39E-04	1.11E-02	0.617	Darc
Darc	13349	8.87E-06	6.77E-04	1.791	

Table S1 continues on the following page

























**Table S1** (continued)

B230217O12Rik	320879	1.03E-05	7.67E-04	-2.257	9 days embryo whole body cDNA, RIKEN full-length enriched library, clone:D030014C21 product:unclassifiable, f
Wscd2	320916	6.37E-07	8.35E-05	-2.403	WSC domain containing 2 (Wscd2), mRNA [NM_177292]
Tmem26	327766	8.38E-04	2.11E-02	-2.968	transmembrane protein 26 (Tmem26), mRNA [NM_177794]
Ppfia2	327814	7.30E-04	1.90E-02	3.180	adult male pituitary gland cDNA, RIKEN full-length enriched library, clone:5330438O12 product:hypothetical prote
Slc39a9	328133	2.23E-04	8.37E-03	-2.916	solute carrier family 39 (zinc transporter), member 9, mRNA (cDNA clone IMAGE:30536025), partial cds. [BC072
Mast4	328329	1.43E-04	6.13E-03	3.192	bone marrow stroma cell CRL-2028 SR-4987 cDNA, RIKEN full-length enriched library, clone:G431004F08 produ
Apol11b	328563	2.16E-03	4.03E-02	-2.068	apolipoprotein L 11b (Apol11b), mRNA [NM_001143686]
D430006K04	328861	4.68E-04	1.38E-02	-1.693	13 days embryo lung cDNA, RIKEN full-length enriched library, clone:D430006K04 product:hypothetical protein, I
A1847670	330050	2.71E-06	2.76E-04	-2.226	expressed sequence A1847670 (A1847670), mRNA [NM_177869]
BC038925	330216	5.47E-04	1.55E-02	-1.217	cDNA sequence BC038925 (BC038925), mRNA [NM_177878]
Fbxo41	330369	1.05E-03	2.49E-02	-2.155	F-box protein 41 (Fbxo41), mRNA [NM_001001160]
Lphn1	330814	3.58E-04	1.16E-02	-1.744	latrophilin 1 (Lphn1), mRNA [NM_181039]
Slc7a6	330836	8.91E-08	1.69E-05	-2.887	solute carrier family 7 (cationic amino acid transporter, y+ system), member 6 (Slc7a6), mRNA [NM_178798]
Hcn4	330953	1.73E-03	3.47E-02	1.331	hyperpolarization-activated, cyclic nucleotide-gated K+ 4 (Hcn4), mRNA [NM_001081192]
Cntln	338349	5.69E-04	1.58E-02	-1.781	centelin, centrosomal protein (Cntln), transcript variant 1, mRNA [NM_175275]
Ust	338362	2.35E-04	8.73E-03	3.231	uronid-2-sulfotransferase (Ust), mRNA [NM_177387]
A730011L01Rik	338371	2.71E-03	4.78E-02	0.894	RIKEN cDNA A730011L01 gene (A730011L01rik), mRNA [NM_177394]
Egfl7	353156	8.57E-04	2.14E-02	0.852	EGF-like domain 7 (Egfl7), transcript variant a, mRNA [NM_178444]
Muc6	353328	4.20E-04	1.29E-02	2.038	mucin 6, gastric (Muc6), mRNA [NM_181729]
Trim46	360213	1.61E-04	6.66E-03	1.624	tripartite motif-containing 46 (Trim46), transcript variant 2, mRNA [NM_183037]
Txlnb	378431	1.97E-10	1.13E-07	-2.984	taxilin beta (Txlnb), mRNA [NM_138628]
Fastkd5	380601	1.22E-05	8.73E-04	-2.045	FAST kinase domains 5 (Fastkd5), mRNA [NM_198176]
Intu	380614	5.14E-05	2.77E-03	1.574	inturned planar cell polarity effector homolog (Drosophila) (Intu), mRNA [NM_175515]
Ccnj1	380694	2.00E-04	7.82E-03	1.728	cyclin J-like (Ccnj1), mRNA [NM_001045530]
AI324046	380795	2.43E-06	2.54E-04	-3.425	mRNA for mFLJ00385 protein [AK131185]
Fam82a1	381110	9.71E-09	2.54E-06	-3.138	family with sequence similarity 82, member A1 (Fam82a1), mRNA [NM_201361]
Tmem151a	381199	4.11E-04	1.27E-02	1.545	transmembrane protein 151A (Tmem151a), mRNA [NM_001001885]
Als2cr4	381259	1.11E-11	1.03E-08	-4.077	amyotrophic lateral sclerosis 2 (juvenile) chromosome region, candidate 4 (Als2cr4), transcript variant 2, mRNA [I
Tbc1d2	381605	8.32E-04	2.11E-02	1.313	3 days neonate thymus cDNA, RIKEN full-length enriched library, clone:A630005A06 product:hypothetical Plecks
Ssbp1	381760	1.50E-03	3.16E-02	-1.967	single-stranded DNA binding protein 1 (Ssbp1), transcript variant 1, mRNA [NM_212468]
4922501C03Rik	382090	1.58E-05	1.07E-03	1.922	RIKEN cDNA 4922501C03 gene (4922501C03rik), mRNA [NM_199316]
A830080D01Rik	382252	2.45E-06	2.55E-04	-2.163	RIKEN cDNA A830080D01 gene (A830080D01rik), mRNA [NM_001033472]
Wdr51b	382406	1.70E-04	6.94E-03	3.480	WD repeat domain 51B (Wdr51b), mRNA [NM_027740]
383196	383196	5.86E-04	1.61E-02	2.761	Immunoglobulin Kappa light chain V gene segment [Source:IMGT/GENE-DB
384261	384261	6.35E-05	3.22E-03	-2.032	PREDICTED: hypothetical LOC384261 (LOC384261), mRNA [XM_986220]
Map4k5	399510	1.61E-04	6.66E-03	0.973	mitogen-activated protein kinase kinase kinase 5 (Map4k5), mRNA [NM_201519]
Plxcd1	403178	4.69E-09	1.47E-06	-2.870	phosphatidylinositol-specific phospholipase C, X domain containing 1 (Plxcd1), mRNA [NM_207279]
Iqgap3	404710	2.57E-03	4.60E-02	-0.984	IQ motif containing GTPase activating protein 3 (Iqgap3), mRNA [NM_001033484]
Bex4	406217	3.30E-04	1.09E-02	1.058	brain expressed gene 4 (Bex4), mRNA [NM_212457]
Specc1	432572	5.08E-04	1.47E-02	1.547	sperm antigen with calponin homology and coiled-coil domains 1 (Specc1), mRNA [NM_001029936]
EG434025	434025	6.75E-05	3.40E-03	-1.959	anti-DNA antibody light chain variable region mRNA, partial cds [U88675]
Gpr62	436090	2.73E-06	2.77E-04	3.407	BY714829 RIKEN full-length enriched, adult male testis cDNA clone 4930431J04 5'. [BY714829]
Ccin	442829	3.78E-06	3.47E-04	1.933	calicin (Ccin), mRNA [NM_001002787]
Cep170	545389	1.92E-03	3.73E-02	-2.016	centrosomal protein 170 (Cep170), mRNA [NM_001099637]
Zfp551	619331	7.16E-08	1.46E-05	-2.737	zinc finger protein 551 (Zfp551), mRNA [NM_001033820]
Igk-V21-4	626347	6.92E-07	8.83E-05	-4.867	immunoglobulin kappa chain variable 21 (V21-4), mRNA (cDNA clone MGIC:118186 IMAGE:4989625), complete
631105	631105	1.03E-03	2.46E-02	2.795	PREDICTED: similar to fibrillae-associated protein Fap1, transcript variant 1 (LOC631105), mRNA [XM_904722]
ENSMUSG00001632737	632737	2.42E-03	4.39E-02	3.745	PREDICTED: predicted gene, EG666638 (EG666638), mRNA [XM_985112]
Sbp1	638345	3.48E-04	1.14E-02	3.104	spermine binding protein-like (Sbp1), mRNA [NM_001077421]
LOC639988	639988	2.03E-06	2.17E-04	-1.829	PREDICTED: similar to immunoglobulin gamma-chain (LOC639988), mRNA [XM_916675]
LOC640979	640979	5.83E-07	7.81E-05	-2.284	Immunoglobulin heavy chain V gene segment [Source:IMGT/GENE-DB
EG665317	666317	1.07E-05	7.87E-04	-2.330	PREDICTED: predicted gene, EG665317, transcript variant 1 (EG665317), mRNA [XM_979163]
Hmcn2	665700	7.71E-04	1.99E-02	2.569	9 days embryo whole body cDNA, RIKEN full-length enriched library, clone:D030068H01 product:inferred: hemio
EG665756	665756	8.97E-04	2.21E-02	1.872	PREDICTED: predicted gene, EG665756 (EG665756), mRNA [XM_979235]
EG668139	668139	5.74E-04	1.59E-02	-0.958	PREDICTED: predicted gene, EG668139 (EG668139), miss RNA [XR_001627]
Zfp507	668501	2.14E-05	1.36E-03	3.010	zinc finger protein 507 (Zfp507), mRNA [NM_177739]
RP23-212C14.7	670533	1.49E-03	3.15E-02	1.272	keratin associated protein 9 family member (LOC670533), mRNA [NM_001101613]
4732444A12Rik	100015211	3.11E-10	1.66E-07	-3.284	21 days neonate cerebellum cDNA, RIKEN full-length enriched library, clone:G630051C23 product:hypothetical p
ENSMUSG0000100038553	4.41E-10	2.14E-07	-3.215	predicted gene, ENSMUSG0000073540, mRNA (cDNA clone MGIC:14005 IMAGE:3660311), complete cds. [BC	
100042757	100042757	1.89E-04	7.54E-03	2.379	PREDICTED: hypothetical protein LOC100046917 (LOC100046917), mRNA [XM_001477379]
100043468	100043468	5.09E-04	1.47E-02	-1.967	predicted gene, 100043468 (100043468), mRNA [NM_001142957]
LOC100047628	100047628	4.28E-04	1.30E-02	-2.270	Immunoglobulin Kappa light chain V gene segment [Source:IMGT/GENE-DB
LOC100048021	100048021	3.95E-04	1.25E-02	0.731	PREDICTED: similar to Guanine nucleotide-binding protein alpha-12 subunit (G alpha-12) (LOC100048021), mRNA
ENSMUSG0000100126228	7.57E-06	5.94E-04	1.253	adult male testis cDNA, RIKEN full-length enriched library, clone:4933429E06 product:hypothetical protein, full:	

Table S2

**Functional Clustering of Differentially Expressed Genes in VSELs Exposed to Intermittent Hypoxia**

Annotation Cluster 1	Enrichment Score: 6.410687762258607	Number of Genes	P-value	Fold Enrichment
Category	Term			
Biological Process	GO:0007275~multicellular organismal development	204	9.74E-11	1.520
Biological Process	GO:0032502~developmental process	217	1.54E-10	1.486
Biological Process	GO:0048856~anatomical structure development	176	2.88E-09	1.523
Biological Process	GO:0048731~system development	164	1.50E-08	1.520
Biological Process	GO:0048513~organ development	135	3.59E-07	1.525
Biological Process	GO:0009653~anatomical structure morphogenesis	96	2.30E-06	1.619
Biological Process	GO:0030154~cell differentiation	119	5.04E-05	1.425
Biological Process	GO:0048869~cellular developmental process	123	5.46E-05	1.412
Biological Process	GO:0032501~multicellular organismal process	245	1.37E-01	1.063
Annotation Cluster 2	Enrichment Score: 4.409348996268908	Number of Genes	P-value	Fold Enrichment
Category	Term			
Biological Process	GO:0001568~blood vessel development	32	6.00E-06	2.463
Biological Process	GO:0001944~vasculature development	32	9.81E-06	2.404
Biological Process	GO:0048514~blood vessel morphogenesis	27	1.83E-05	2.561
Biological Process	GO:0001525~angiogenesis	20	7.68E-05	2.825
Annotation Cluster 3	Enrichment Score: 3.8059194810335697	Number of Genes	P-value	Fold Enrichment
Category	Term			
Biological Process	GO:0009790~embryonic development	63	1.35E-05	1.766
Biological Process	GO:0043009~chordate embryonic development	45	1.39E-05	2.008
Biological Process	GO:0048598~embryonic morphogenesis	40	1.80E-05	2.093
Biological Process	GO:0048568~embryonic organ development	27	4.84E-04	2.104
Biological Process	GO:0001701~in utero embryonic development	27	2.17E-03	1.899
Biological Process	GO:0009887~organ morphogenesis	43	3.66E-02	1.360
Annotation Cluster 4	Enrichment Score: 2.6233303269471335	Number of Genes	P-value	Fold Enrichment
Category	Term			
Biological Process	GO:0048598~embryonic morphogenesis	40	1.80E-05	2.093
Biological Process	GO:0035113~embryonic appendage morphogenesis	14	1.83E-03	2.711
Biological Process	GO:0030326~embryonic limb morphogenesis	14	1.83E-03	2.711
Biological Process	GO:0035108~limb morphogenesis	14	8.02E-03	2.287
Biological Process	GO:0035107~appendage morphogenesis	14	8.02E-03	2.287
Biological Process	GO:0060173~limb development	14	1.06E-02	2.210
Biological Process	GO:0048736~appendage development	14	1.06E-02	2.210
Annotation Cluster 5	Enrichment Score: 2.5479907939308135	Number of Genes	P-value	Fold Enrichment
Category	Term			
Biological Process	GO:0001822~kidney development	17	1.61E-04	2.984
Biological Process	GO:0001655~urogenital system development	18	1.93E-03	2.316
Biological Process	GO:0001657~ureteric bud development	8	6.18E-03	3.578
Biological Process	GO:0001656~metanephros development	8	3.33E-02	2.591

Table S2 continues on the following page

**Table S2** (continued)

Annotation Cluster 6	Enrichment Score: 2.512425848615364			
Category	Term	Number of Genes	P-value	Fold Enrichment
Biological Process	GO:0048598~embryonic morphogenesis	40	1.80E-05	2.093
Biological Process	GO:0048568~embryonic organ development	27	4.84E-04	2.104
Biological Process	GO:0043583~ear development	14	3.42E-03	2.529
Biological Process	GO:0048562~embryonic organ morphogenesis	18	5.35E-03	2.100
Biological Process	GO:0042471~ear morphogenesis	11	6.76E-03	2.719
Biological Process	GO:0048839~inner ear development	12	6.81E-03	2.561
Biological Process	GO:0042472~inner ear morphogenesis	10	8.71E-03	2.803
Biological Process	GO:0007423~sensory organ development	24	1.05E-02	1.754
Biological Process	GO:0009887~organ morphogenesis	43	3.66E-02	1.360
Annotation Cluster 7	Enrichment Score: 2.432221052606057			
Category	Term	Number of Genes	P-value	Fold Enrichment
Biological Process	GO:0007155~cell adhesion	48	1.35E-03	1.607
Biological Process	GO:0022610~biological adhesion	48	1.40E-03	1.604
Biological Process	GO:0016337~cell-cell adhesion	21	2.68E-02	1.671
Annotation Cluster 8	Enrichment Score: 2.3347226255726903			
Category	Term	Number of Genes	P-value	Fold Enrichment
Biological Process	GO:0035295~tube development	31	7.20E-05	2.206
Biological Process	GO:0001569~patterning of blood vessels	6	7.66E-03	4.696
Biological Process	GO:0035239~tube morphogenesis	18	9.63E-03	1.977
Biological Process	GO:0001763~morphogenesis of a branching structure	14	1.55E-02	2.104
Biological Process	GO:0048754~branching morphogenesis of a tube	11	2.57E-02	2.222
Annotation Cluster 9	Enrichment Score: 2.2522030394510346			
Category	Term	Number of Genes	P-value	Fold Enrichment
Biological Process	GO:0007420~brain development	29	1.53E-03	1.891
Biological Process	GO:0007399~nervous system development	64	4.83E-03	1.408
Biological Process	GO:0007417~central nervous system development	32	8.12E-03	1.629
Biological Process	GO:0030900~forebrain development	17	1.63E-02	1.912
Annotation Cluster 10	Enrichment Score: 2.0995523296663214			
Category	Term	Number of Genes	P-value	Fold Enrichment
Biological Process	GO:0019216~regulation of lipid metabolic process	10	3.31E-03	3.239
Biological Process	GO:0019218~regulation of steroid metabolic process	6	5.18E-03	5.123
Biological Process	GO:0050810~regulation of steroid biosynthetic process	5	8.64E-03	5.870
Biological Process	GO:0046890~regulation of lipid biosynthetic process	5	2.70E-02	4.269
Annotation Cluster 11	Enrichment Score: 2.0748660760971993			
Category	Term	Number of Genes	P-value	Fold Enrichment
Biological Process	GO:0035295~tube development	31	7.20E-05	2.206
Biological Process	GO:0030324~lung development	13	1.48E-02	2.200
Biological Process	GO:0030323~respiratory tube development	13	1.69E-02	2.161
Biological Process	GO:0060541~respiratory system development	13	3.23E-02	1.969
Biological Process	GO:0008543~fibroblast growth factor receptor signaling pathway	5	7.26E-02	3.131

Table S2 continues on the following page

**Table S2** (continued)

Annotation Cluster 12	Enrichment Score: 1.8887932893479804			
Category	Term	Number of Genes	P-value	Fold Enrichment
Biological Process	GO:0001558~regulation of cell growth	15	3.39E-04	3.063
Biological Process	GO:0045792~negative regulation of cell size	9	6.52E-03	3.190
Biological Process	GO:0030308~negative regulation of cell growth	8	1.15E-02	3.197
Biological Process	GO:0045926~negative regulation of growth	9	3.42E-02	2.381
Biological Process	GO:0008361~regulation of cell size	11	6.13E-02	1.913
Biological Process	GO:0032535~regulation of cellular component size	14	8.76E-02	1.633
Annotation Cluster 13	Enrichment Score: 1.8348372706488445			
Category	Term	Number of Genes	P-value	Fold Enrichment
GOTERM_MF_ALL	GO:0008034~lipoprotein binding	6	4.64E-03	5.239
GOTERM_MF_ALL	GO:0005041~low-density lipoprotein receptor activity	4	1.06E-02	8.150
GOTERM_MF_ALL	GO:0030169~low-density lipoprotein binding	4	3.06E-02	5.642
GOTERM_MF_ALL	GO:0030228~lipoprotein receptor activity	4	3.06E-02	5.642
Annotation Cluster 14	Enrichment Score: 1.830345700823631			
Category	Term	Number of Genes	P-value	Fold Enrichment
Biological Process	GO:0007389~pattern specification process	28	2.54E-03	1.852
Biological Process	GO:0003002~regionalization	20	1.98E-02	1.755
Biological Process	GO:0009952~anterior/posterior pattern formation	14	6.41E-02	1.719
Annotation Cluster 15	Enrichment Score: 1.5577264652830227			
Category	Term	Number of Genes	P-value	Fold Enrichment
Biological Process	GO:0001501~skeletal system development	26	9.88E-03	1.714
Biological Process	GO:0060348~bone development	13	2.30E-02	2.069
Biological Process	GO:0001503~ossification	12	2.52E-02	2.126
Biological Process	GO:0001649~osteoblast differentiation	6	1.03E-01	2.398

